New methodology for the experimental determination of the consumption speed in spherical vessels

A. Lefebvre[1,*], H. Larabi[1], V. Moureau[1], E. Varea[1], V. Modica[1], B. Renou[1]

[1] CORIA UMR 6614 CNRS,
Avenue de l'Université, BP 08,
76801 Saint Etienne du Rouvray, France

Abstract

Laminar burning velocity is an essential quantity for both combustion modeling and kinetic scheme validation and improvement. Among the different techniques, experimental facility using a spherical flame is generally chosen as it offers flexibility in terms of initial conditions. Experimental laminar burning velocity data are generally produced and compared to the 1D planar case, which necessitates an extrapolation procedure to zero stretch. A direct comparison of experimental data with DNS can avoid this problem [1]. For spherical flame configurations, only the propagation speed and the displacement speed relative to the fresh gases can be measured without any ambiguity [2]. Therefore the challenges remain in determining experimentally the burning velocity based on the integral of the reaction rate, which is the consumption speed. While deriving the equations in spherical coordinates, various expressions for the consumption speed can be found [3–5]. Recent studies [2] have shown that the velocity field ahead of the flame front was accessible using specific tomography algorithms. Applying the mass conservation equation on a control volume, it is possible to access the value of the instantaneous fresh gases density while the flame expands, which can be linked to the consumption speed. The objectives of the present work are to propose a new experimental approach to estimate directly the consumption speed for spherical flames and validate it with direct numerical simulations including detailed chemistry. Finally experimental results of this new methodology are presented.

Introduction

The laminar burning velocity (LBV), U_n^0, is a fundamental property which is defined as the speed relative to the unburned gases, of a planar, one-dimensional, stationary, adiabatic and unstretched flame front [3]. It is an important quantity for kinetic schemes validation and improvement, and a key parameter for the modeling of complex combustion phenomena: flame stabilization, extinction, scaling of turbulent flames [6–8]. An accurate determination of this velocity is essential. In a one dimensional approach, the LBV is equal to the consumption speed S_c^0 linked to the mass of species k that is converted in the flame front and defined by the reaction rate $\dot{\omega}_k$ [7]

$$S_c^0 = \frac{1}{\rho_u (Y_k^b - Y_k^u)} \int_{-\infty}^{+\infty} \dot{\omega}_k dx, \tag{1}$$

where ρ_u is the fresh gases density and Y_k is the mass fraction of species k for the fresh and burned gases, superscript ^{u} and ^{b}, respectively.

For the experimental determination of the LBV, spherical expanding flames (SEF) are extensively used since they offer flexibility in terms of initial conditions (pressure, temperature and equivalence ratio). However, since the flame front is affected by curvature and strain (stretch, κ) effects, extrapolation procedure to zero stretch is needed to get the unstretched laminar burning velocity [9, 10]. Uncertainties and impact of the extrapolation procedure are not explored in the present work, which is focused on experimental techniques to measure the laminar burning velocity based on a novel approach. From theoretical analysis, different formulations can be derived for the LBV. Hereafter, the mean formulae found in literature are presented. In SEF configuration, one can define:

- the propagation speed

$$S_f = \frac{dR_f}{dt} - u_b \approx \frac{dR_f}{dt},$$

where R_f is the flame front radius and u_b the burned gas velocity. The burned gas are assumed inert during the flame propagation. This velocity is defined in the laboratory frame of reference and is predominantly used to determine the LBV [4, 11–13] by the following approximation

$$S_l^0 = \frac{\rho_b^{eq}}{\rho_u} \, lim_{\kappa \to 0} \left(\frac{dR_f}{dt} \right), \tag{2}$$

where ρ_b^{eq} is the burned gases density commonly estimated with adiabatic equilibrium solvers and ρ_u is the fresh gases density at the initial state.

- the displacement speed

$$U_n = \frac{dR_f}{dt} - u_g, \tag{3}$$

where u_g is the fresh gases velocity at the entrance of the flame front. This velocity expresses the fresh gases velocity in the flame front frame of reference. As a consequence it is a kinematic definition of the LBV, which only requires extrapolation to zero stretch.

- the consumption speed

$$S_c = \frac{1}{\rho_u \left[Y_k^b - Y_k^u \right] R_f^2} \int_0^{R_0} \dot{\omega}_k r^2 dr \tag{4}$$

This expression is the definition in spherical coordinates of the consumption speed for any species k considering a one-step reaction: reactants (f) $\rightarrow$ products (P), where k is either reactant or product.

Experimentally, Eq. 2 is easy to use since it only requires the propagation speed $\frac{dR_f}{dt}$ easily accessible by recording the temporal evolution of the flame front location with classical optical methods (Schlieren, shadowgraphy or tomography). However many biases can be introduced:

- the burned gases are not necessarily at the equilibrium, especially at low pressure [2].

*Corresponding author: lefebvra@coria.fr

- stretch can affect the burned gases temperature according to the Lewis number of the mixture [14], especially at the early stages of the flame propagation. Recently it has been shown that this bias is non-negligible [5].
- the amount of burned gases within the flame front is not negligible and must be taken into account. Note that this is not the case for this Eq. 3 which is developed for infinitely thin flame. This was first shown by Dowdy et al. [15], and Poinsot et al. [16] developed a model to take into account the burned gases mass ρY_P (or the fresh gases mass ρY_F) across the flame front.

Therefore, this method is not fully recommended to determine the LBV even if good results are obtained for U_n^0, the errors can be quite large on Markstein length ℓ_c values [5].

On the contrary, Eq. 3 is free of assumptions and can be directly determined by a specific measurement technique using high-speed tomographic records. This technique has been validated for various gaseous or liquid fuels [2, 17]. Moreover recent collaborative works [1] present this method as a good candidate for an accurate determination of the LBV as it is not influenced by radiative effects nor by the burned gases equilibrium state assumption.

Concerning Eq. 4, the source term $\dot{\omega_k}$ can not be determined experimentally. Therefore, one should develop Eq. 4 with measurable parameters. Many strategies have been investigated for an experimental determination of S_c in the context of spherical expanding flames [2, 4, 5, 18, 19]. These approaches are based on models, which are limiting the accuracy.
In the end, there are, to the authors' knowledge, no available way to determine experimentally the consumption speed with accuracy in SEF configuration. Therefore, the objectives of this paper are twofold:

- Propose a new methodology to determine the consumption speed from experimental data,
- Validate the new methodology using DNS calculation,

Definition of the consumption speed

As mentioned before, the consumption speed, Eq. 4 can not be determined experimentally, since the source term $\dot{\omega_k}$ is unknown. Nevertheless, integrating the species transport equation along the domain yields:

$$\int_0^{R_0} \dot{\omega_k} r^2 dr = \frac{d}{dt} \int_0^{R_0} \rho Y_k r^2 dr \tag{5}$$

and Eq. 4 can be reformulated as:

$$S_c = \frac{1}{\rho_u \left[Y_k^b - Y_k^u\right] R_f^2} \frac{d}{dt} \int_0^{R_0} \rho Y_k r^2 dr. \tag{6}$$

From Eq. 6, the mass of the species k and ρY_k through the volume chamber are needed. One can define R_{eq} as a radius such as all the fresh gases are included between R_{eq} and R_0. Then the fresh gas mass is defined by

$$M_f = \rho_u Y_f^u (\frac{4}{3}\pi R_0^3 - \frac{4}{3}\pi R_{eq}^3). \tag{7}$$

Combining Eq. 7 with Eq. 6, and assuming:

- on the fresh side ($R_{eq} < r < R_0$), the density $\rho = \rho_u$ is homogeneous,
- the fuel mass fraction $Y_F^u = 1$ and
- on the burned side ($0 < r < R_{eq}$) no fresh gases remains, inducing that the mass fraction of fuel is $Y_F^b = 0$,

Eq. 6 yields

$$S_c = \frac{1}{4\pi\rho_u (Y_f^b - Y_f^u) R_{eq}^2} \frac{d}{dt} \left(\rho_u Y_f^u (\frac{4}{3}\pi R_0^3 - \frac{4}{3}\pi R_{eq}^3) \right). \tag{8}$$

Therefore, the consumption speed is as follow

$$S_c = \frac{dR_{eq}}{dt} - \frac{(R_0^3 - R_{eq}^3)}{3R_{eq}^2} \frac{1}{\rho_u} \frac{d\rho_u}{dt}. \tag{9}$$

It is worth noting that no assumptions have been introduced. However, to determine the consumption speed, several quantities are mandatory:

- R_0, the internal chamber radius, which can be easily measured in experimental devices,
- R_{eq}, the equivalent flame radius of a sphere containing all the mass of fresh gases present into the vessel, and
- ρ_u, the fresh gas density.

From Eq. 9, Bonhomme et al. [5] suggested to combine both the temporal evolution of the flame radius and the internal pressure chamber $P(t)$ in order to estimate the consumption speed. Assuming an isentropic compression of the fresh gases, Bonhomme et al. [5] defined the consumption speed as

$$S_c = \frac{dR_f}{dt} - \frac{(R_0^3 - R_f^3)}{3R_f^2} \frac{1}{\gamma_u P} \frac{dP}{dt}. \tag{10}$$

The numerical analysis of Bonhomme et al. [5] showed that the inherent difficulties of Eq. 2 mentioned before can be overcome since Eq. 10 only requires the time radius evolution and the pressure signal. Nevertheless, as explained by Bradley et al. [3], the experimental values of laminar burning velocity obtained from this methodology might be not accurate enough, since this formula is based on the difference of two large numbers. This means that the accuracy of the experimental pressure signal must be excellent to avoid any noise during the time derivative computation.

To cope this problem, a direct measurement of the fresh gas density evolution during the flame propagation is necessary. The present work describes a novel experimental procedure to access to an accurate value of the desired quantity ρ_u.

A new tool to determine the fresh gas density of freely propagating spherical expanding flames

The aim of this section is to present a new methodology to determine the temporal evolution of the fresh gas density from parameters which can be measured from experimental tomographic records.
The mass conservation equation is defined on a material volume without sources or holes by

$$\frac{d}{dt} \int_{V_m(t)} \rho dV = 0. \tag{11}$$

Following the transport theorem on a material volume $V_m(t)$ [20], Eq. 11 yields

$$\frac{d}{dt} \int_{V_m} \rho \, dV = \int_{V_m} \frac{\partial \rho}{\partial t} dV + \oint_{A_m} \rho \vec{U}.\vec{n} dA = 0 \tag{12}$$

with $\vec{U}$ the local fluid velocity and $\vec{n}$ the normal to the volume. Considering an arbitrary control volume $V_a(t) = V_m(t)$, Fig. 1, located in between $r = X$ and $r = R_0$,

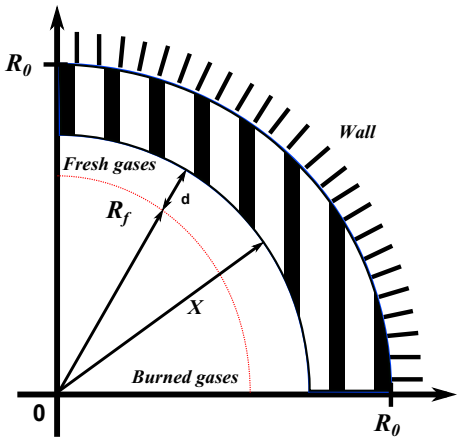

Figure 1: Diagram of an arbitrary control volume.

Eq. 12 yields to [20]:

$$\frac{d}{dt}\int_{V_m}\rho\,dV=\frac{d}{dt}\int_{V_a}\rho\,dV+\oint_{A_a}\rho\left(\vec{U}-\vec{\dot{X}}\right).\vec{n}dA=0 \tag{13}$$

with $\dot{X}$ the local velocity of the area $A_a(t)$. Viewed in the projection onto the radial axis, Eq. 13 is

$$\frac{d}{dt}\int_{V_m}\rho\,dV=\frac{d}{dt}\int_{V_a}\rho\,dV-\oint_{A_a}\rho\left(U-\dot{X}\right)dA=0. \tag{14}$$

Integrating Eq. 14 between time t^n and t^{n+1} leads to

$$\frac{\left(\int\rho\,dV\right)^{n+1}-\left(\int\rho\,dV\right)^{n}}{t^{n+1}-t^n}-\oint_{\Sigma^{n+1/2}}\rho\left(U-\dot{X}\right)dA=0. \tag{15}$$

Assuming that ρ, U and $\dot{X}$ are homogeneous at each time step and introducing as a first approximation

$$\rho^{n+1/2}=\frac{\rho^{n+1}+\rho^n}{2}, \tag{16}$$

the temporal fresh gas density evolution is

$$\rho^{n+1}=\rho^n\times\frac{\left[\frac{R_0^3-(X^n)^3}{3\Delta t}+\frac{1}{2}\left(\frac{X^{n+1}+X^n}{2}\right)^2\left(U^{n+1/2}-\frac{X^{n+1}-X^n}{\Delta t}\right)\right]}{\left[\frac{R_0^3-(X^{n+1})^3}{3\Delta t}-\frac{1}{2}\left(\frac{X^{n+1}+X^n}{2}\right)^2\left(U^{n+1/2}-\frac{X^{n+1}-X^n}{\Delta t}\right)\right]} \tag{17}$$

Therefore, one can determine the fresh gas density evolution if the following quantities:

- X the position of the control volume moving surface, and
- U the fluid velocity at the position X,

can be measured

Validation of the methodology

1. *Numerical procedure*

In the present work, simulations are conducted with the finite-volume code YALES2 [21], a low-Mach number Large-Eddy Simulation (LES) solver for reactive flows based on unstructured meshes. Combustion is taken into account through finite-rate chemistry in order to provide a realistic description of both thermodynamics of the mixture and transport properties of individual species. The partial density of each species present in the mixture are transported along with the density, momentum and sensible enthalpy equations. The diffusion velocities are obtained using the Hirschfelder and Curtiss approximation [7]. To avoid a drastic time step limitation due to the chemical time scales, a splitting algorithm is implemented in YALES2, which consists in integrating separately the chemistry with a stiff Ordinary Differential Equation solver from the transport and diffusion terms.

The simulation domain is a solid angle of 1 degree and radius $R_0 = 82.5\,mm$. It is composed of $330\,k$ elements refined up to $20\,\mu m$ in the flame front. The size and geometry of this domain are comparable to the experimental device used in the present study. This mesh resolution was found enough to accurately predict the laminar flame speed and the major species profiles. Periodic boundary conditions are applied on faces perpendicular to the flame propagation direction. An adiabatic wall is fixed at the extremity of the domain. Simulations were performed with the *GRI-mech 3.0* mechanism, which counts 53 species and 325 reversible reactions. Fresh gases are initially at a temperature of $300\,K$ and a pressure of $1\,atm$. The flow is considered adiabatic and the flame ball is ignited with a small pocket of burned gases.

2. *Equations validity with experimental data consideration*

The resolution of Eq. 9 requires several parameters. On the left hand side, it requires the equivalent radius R_{eq}. On the right hand side, the fluid velocity U at the edge Σ of a control volume and the position of this edge X are needed. From experiments using tomographic record technique, the flame radius is defined at the droplet evaporation isotherm R_{tomo}. The latter does not necessarily corresponds to the radius R_{eq}. Figure 2 represents the normalized difference $\frac{R_{eq}-R_{tomo}}{R_{eq}}$ as a function of time for a simulated stoichiometric CH_4/air flame.

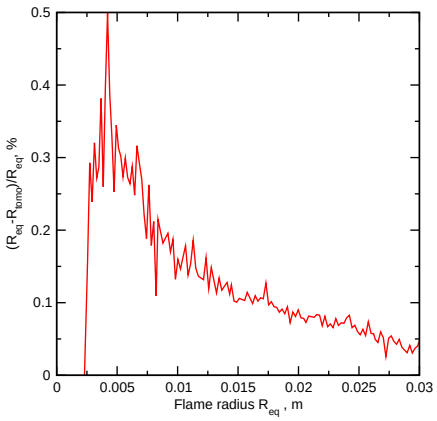

Figure 2: Normalized difference $\frac{R_{eq}-R_{tomo}}{R_{eq}}$ as a function of time for a stoichiometric CH_4/air flame simulated with YALES2 code.

From numerical results of Fig. 2, the difference between the idealistic radius R_{eq} and the measurable flame radius R_{tomo} is less than 0.5%, and quickly decreases to be less than 0.15% in the radius range corresponding to experimental measurement:

$8 < R < 25\,mm$. As a consequence, one can assumed that $R_{eq} = R_{tomo}$ in this case.
In the present methodology, the temporal fresh gas density evolution is evaluated from Eq. 17, which requires the position X and velocity U of the fluid at this position. Figure 3 compares the fresh gases density extracted from simulations to the fresh gas density calculated by this equation with numerical parameters X and U comparable to the experiments. It can be seen

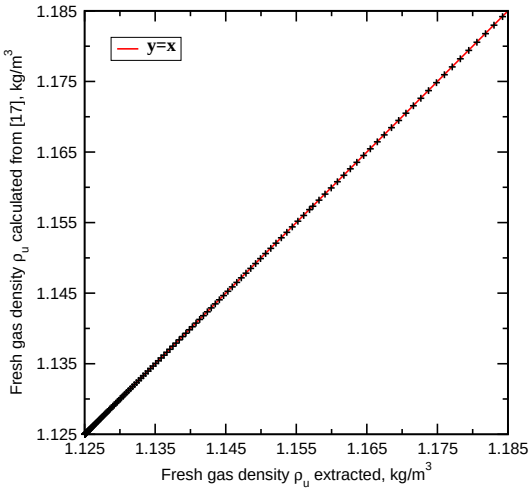

Figure 3: Comparison of the fresh gases density extracted from simulations to the fresh gas density calculated by Eq. 17, for a stoichiometric CH_4/air flame.

that there is no difference between fresh gas densities directly extracted from computed density fields and these from calculations using Eq. 17. Then the evaluation of the density using Eq. 17 is validated. Experimentally, parameters X and U are measurable thanks to laser tomography technique combined with a inhouse developed post-processing software [2] and are the same than in simulation.

Actually, Eq. 9 is experimentally accessible as :

$$S_c = \frac{dR_{tomo}}{dt} - \frac{(R_0^3 - R_{tomo}^3)}{3R_{tomo}^2}\frac{1}{\rho_u}\frac{d\rho_u}{dt}, \qquad (18)$$

where ρ_u is evaluated with Eq. 17. The validity of the procedure is checked in Fig. 4, where Eq.4, Eq.9 and Eq.18 are compared. All data come from simulations. Good agreement is obtained even though the consumption speed from Eq. 9 and Eq. 18 shows a scattered trace. This problem could come from the time derivative calculation of $\frac{dR}{dt}$ and $\frac{d\rho_u}{dt}$, which is highly sensitive due to very small variation in radius and density data.

The next section presents the application of this new methodology using experimental data. Measurement accuracy and repeatability is also discussed.

Experimental results

The measurement technique used in the present work is the tomographic records. It is performed at an acquisition rate of 5000 Hz and allows to determine the flame front radius R_{tomo} with a subpixel accuracy. Moreover a PIV post-processing enables to resolve the fresh gas velocity profile ahead of the flame front until its maximal value at the entrance of the flame front U_g. The figure 5 shows the velocity profile ahead of the flame

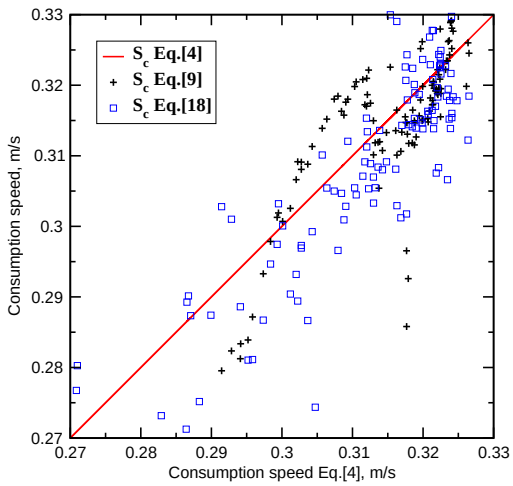

Figure 4: Comparaison of models to determine the LBV: Eq.4, Eq.9 and Eq.18, for a stoichiometric CH_4/air flame.

front determined from tomographic records, of a stoichiometric CH_4/air flame at atmospheric pressure and initial temperature $T = 300\ K$. Further explanations on the profile extraction

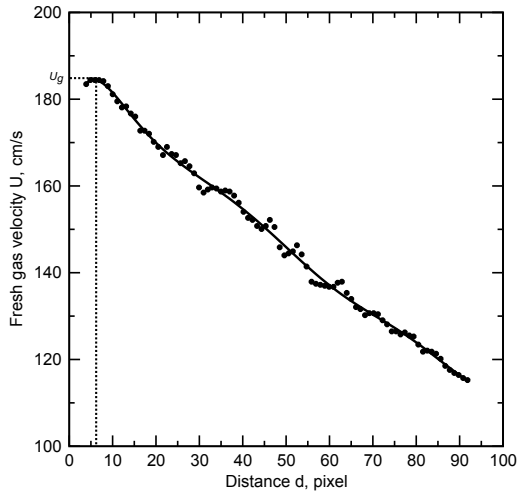

Figure 5: Profile of the normal component of the fresh gas velocity with a 10^{th} order polynomial fit of a stoichiometric CH_4/air flame 7.2 ms after ignition.

technique are given in [2]. The velocity U at the distance d of the flame front, equal to the position X (see Fig.1), is then accessible. During the post-processing, d is a distance from the flame front set by the user which ensures that in the region between $R_{tomo} + d$ and R_0, the fresh gases density is spatially homogeneous. To ensure the reliability of this method, the post-processing has been done for several distances ahead of the flame front: $d \in [70; 90]$ pxl for a stoichiometric CH_4/air flame. As a consequence, the post-processing made on an arbitrary volume can be validated in this range. In the later part of this work, the selected value of d has been fixed to $d = 80pxl$.

To test the repeatability of measurements, Fig.6 shows the term $\frac{1}{\rho_u}\frac{d\rho_u}{dt}$ evaluated from three different stoichiomet-

ric CH_4/air flame tests, superimposed and compared to the simulation. The comparison made in this figure demonstrates that measurements are repeatable but shows a slight drift with the simulation results. This drift is confirmed in Fig.7 which compares the consumption speed determined experimentally with Eq.18 to the one calculated numerically with Eq.4. Furthermore, the experimental and numerical consumption speeds for stretch greater than $450s^{-1}$ are totally different. In this range of stretch rate, the difference could be explained by an ignition effect in the experiment causing a faster propagation flame speed.

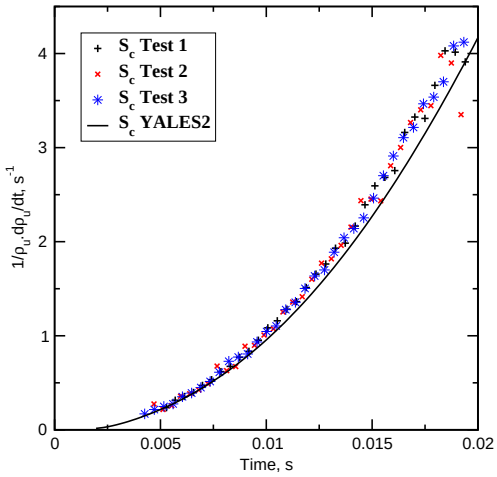

Figure 6: Comparison of $\frac{1}{\rho_u}\frac{d\rho_u}{dt}$ calculated from three different tests superimposed and the DNS of YALES2 code, for a stoichiometric CH_4/air flame at atmospheric pressure and initial temperature $T = 300\ K$.

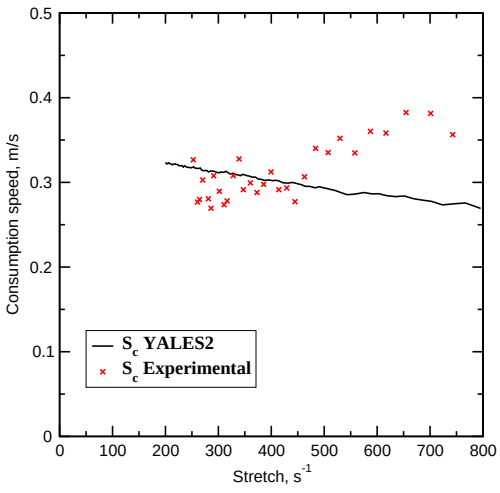

Figure 7: Comparaison of the consumption speed extracted from DNS or determine in experiment as function of the stretch rate, for a stoichiometric CH_4/air flame at atmospheric pressure and initial temperature $T = 300\ K$.

The results presented here come from a work in progress. A further work must be done on the post-processing methodology.

Otherwise, to test Eq.10, the pressure signal is recorded during experiments, with a high sensitive pressure sensor *Kistler* 7001. Since Eq.10 and Eq.9 are linked by the isentropic compression assumption, a comparison between the two terms: $(1/\rho_u)d\rho_u/dt$ and $1/(\gamma_u P)dP/dt$ is relevant and enables to compare the measurement accuracy of these two methods. Figure 8 represents the temporal evolution of these two terms. It

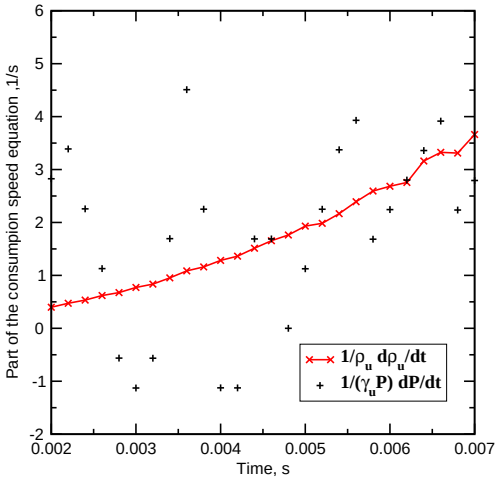

Figure 8: Comparison between $1/(\gamma_u P)dP/dt$ and $\frac{1}{\rho_u}\frac{d\rho_u}{dt}$ calculated from experimental data of a stoichiometric CH_4/air flame at atmospheric pressure and initial temperature $T = 300\ K$.

is clear on Fig.8 that it is impossible to use raw pressure signal to evaluate Eq.10 because the term $1/(\gamma_u P)dP/dt$ is too noisy. Consequently, Eq.10 seems not adapted to determine experimentally the LBV. Especially if the fresh gases density is accessible with a better accuracy.

To summarize, the figure 9 presents the three definitions of the LBV that can be measured from tomographic records as a function of the stretch rate. They are plotted in stretch range of $[240\ 500]\ s^{-1}$, corresponding to a flame radius: $0.009 < R < 0.024$ m. A linear extrapolation is also presented on the two models: Sl (Eq.2) and U_n (Eq.3). N.B: for the studied fuel and thermodynamical conditions, a linear extrapolation is a valid extrapolation model to estimated the LBV from stretch measurements. Finally, the new methodology presented in this study requires additional work to be completely validated. Nevertheless, it could be an alternative to the classical method S_l (Eq.2) to determine the LBV, which can introduce significant errors for complex fuels, and allows to make direct comparisons between experiments and simulations, as the model U_n [1].

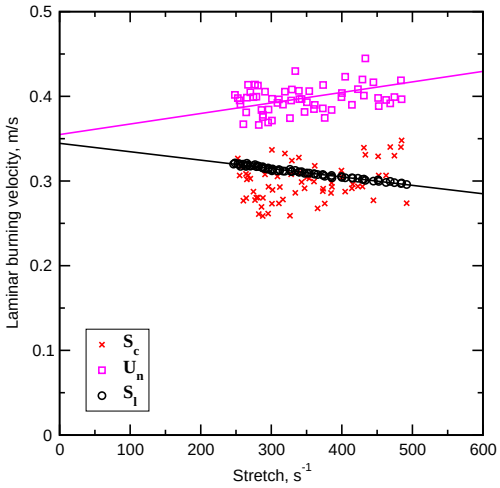

Figure 9: Superposition of the three models of LBV experimentally accessible for a stoichiometric CH_4/air flame at atmospheric pressure and initial temperature $T = 300\ K$.

Conclusion

In conclusion, the present paper proposes a new methodology to determine experimentally the consumption speed, based on the determination of the temporal evolution of the fresh gases density. Thanks to three dimensional direct numerical simulation, executed with the inhouse code *YALES2* [21], it could be demonstrated the validity of this technique with measurable parameters in experiments, such as the flame radius extractable from tomographic records: R_{tomo} or the velocity profile ahead of the flame front. However, the numerical study has highlighted a high noise sensitivity of this new methodology. This observation has been confirmed by the application of this methodology on experimental measurements. Therefore, this new methodology requires additional work on the data post-processing precision. Furthermore it has been show that the methodology proposes by Bonhomme et al. [5], which is a development of the present methodology with an isentropic compression assumption, could not be exploitable with experimental data since the pressure measurement and treatment, even with high sensitive sensor, is even more noisy compare to the fresh gases density evaluation.

Acknowledgements

This work was supported by the INSA of Rouen (France). Dr. Ghislain Lartigue is also acknowledged for his support.

References

[1] J. Jayachandran, A. Lefebvre, R. Zhao, F. Halter, E. Varea, B. Renou, F. N. Egolfopoulos, Proceedings of the Combustion Institute 35 (2015) 695–702.

[2] E. Varea, V. Modica, A. Vandel, B. Renou, Combustion and Flame 159 (2012) 577–590.

[3] G. E. Andrews, D. Bradley, Combustion and Flame 18 (1972) 133–153.

[4] D. Mitcheson, B. A., Combustion and Flame 26 (1976) 201 – 217.

[5] A. Bonhomme, L. Selle, T. Poinsot, Combustion and Flame 160 (2013) 1208–1214.

[6] D. Veynante, L. Vervisch, Progress in Energy and Combustion Science 28 (2002) 193–266.

[7] T. Poinsot, D. Veynante, Theoretical and Numerical Combustion, Third Edition (www.cerfacs.fr/elearning), 2011.

[8] E. Ranzi, A. Frassoldati, R. Grana, A. Cuoci, T. Faravelli, A. P. Kelley, C. K. Law, Progress in Energy and Combustion Science 38 (2012) 468–501.

[9] A. P. Kelley, C. K. Law, Combustion and Flame 156 (2009) 1844–1851. 0010-2180 doi: DOI: 10.1016/j.combustflame.2009.04.004.

[10] F. Halter, T. Tahtouh, C. Mounaim-Rousselle, Combustion and Flame 157 (2010) 1825–1832.

[11] M. I. Hassan, K. T. Aung, G. M. Faeth, Combustion and Flame 115 (1998) 539–550.

[12] F. Halter, C. Chauveau, N. Djebaili-Chaumeix, I. Gokalp, Proceedings of the Combustion Institute (2005) 201–208.

[13] P. Brequigny, G. Dayma, F. Halter, C. MounaÃŕm-Rousselle, T. Dubois, P. Dagaut, Proceedings of the Combustion Institute 35 (2015) 703–710.

[14] C. Law, Proceedings of the Combustion Institute 22 (1989) 1381–1402.

[15] D. Dowdy, D. Smith, S. Taylor, Proceedings of the Combustion Institute (1990) 325 – 332.

[16] T. Poinsot, Combustion and Flame 113 (1998) 279–284.

[17] E. Varea, V. Modica, B. Renou, A. M. Boukhalfa, Proceedings of the Combustion Institute 34 (2013) 735–744.

[18] E. Fiock, C. Marvin, Chemical Reviews 21 (1937) 367–387.

[19] D. Bradley, P. H. Gaskell, X. J. Gu, Combustion and Flame 104 (1996) 176–198.

[20] S. Candel, Mecanique des fluides, DUNOD, 1995.

[21] T. CORIA CFD, 2015. Http://www.coria-cfd.fr.